



**HAL**  
open science

## **IGF-1 activates hEAG K<sup>+</sup> channels through an Akt-dependent signaling pathway in breast cancer cells: Role in cell proliferation**

Anne-Sophie Borowiec, Frédéric Hague, Noria Harir, Stéphanie Guénin, François Guérineau, Fabrice Gouilleux, Morad Roudbaraki, Kaiss Lassoued, Halima Ouadid-Ahidouch

### ► To cite this version:

Anne-Sophie Borowiec, Frédéric Hague, Noria Harir, Stéphanie Guénin, François Guérineau, et al.. IGF-1 activates hEAG K<sup>+</sup> channels through an Akt-dependent signaling pathway in breast cancer cells: Role in cell proliferation. *Journal of Cellular Physiology*, 2007, 212 (3), pp.690-701. 10.1002/jcp.21065 . hal-02424608

**HAL Id: hal-02424608**

**<https://univ-tours.hal.science/hal-02424608>**

Submitted on 30 Oct 2021

**HAL** is a multi-disciplinary open access archive for the deposit and dissemination of scientific research documents, whether they are published or not. The documents may come from teaching and research institutions in France or abroad, or from public or private research centers.

L'archive ouverte pluridisciplinaire **HAL**, est destinée au dépôt et à la diffusion de documents scientifiques de niveau recherche, publiés ou non, émanant des établissements d'enseignement et de recherche français ou étrangers, des laboratoires publics ou privés.

# IGF-1 Activates hEAG K<sup>+</sup> Channels Through an Akt-Dependent Signaling Pathway in Breast Cancer Cells: Role in Cell Proliferation

ANNE-SOPHIE BOROWIEC,<sup>1</sup> FRÉDÉRIC HAGUE,<sup>1</sup> NORIA HARIR,<sup>2</sup> STÉPHANIE GUÉNIN,<sup>3</sup> FRANÇOIS GUERINEAU,<sup>4</sup> FABRICE GOUILLEUX,<sup>2</sup> MORAD ROUDBARAKI,<sup>5</sup> KAISS LASSOUED,<sup>2</sup> AND HALIMA OUADID-AHIDOUCH<sup>1\*</sup>

<sup>1</sup>Laboratoire de Physiologie Cellulaire, EA 2086, Faculté des Sciences, Université de Picardie Jules Verne, Amiens, France

<sup>2</sup>Laboratoire d'Immunologie, INSERM E351, Faculté de Médecine, Université de Picardie Jules Verne, Amiens, France

<sup>3</sup>Centre de Ressources Régionales en Biologie Moléculaire, Université Picardie Jules Verne, Amiens, France

<sup>4</sup>Laboratoire de Génomique Fonctionnelle des Plantes, Université Picardie Jules Verne, Amiens, France

<sup>5</sup>Laboratoire de Physiologie Cellulaire, INSERM U800, USTL, Villeneuve d'Ascq, France

Previous work from our laboratory has shown that human ether à go-go (hEAG) K<sup>+</sup> channels are crucial for breast cancer cell proliferation and cell cycle progression. In this study, we investigated the regulation of hEAG channels by an insulin-like growth factor-1 (IGF-1), which is known to stimulate cell proliferation. Acute applications of IGF-1 increased K<sup>+</sup> current-density and hyperpolarized MCF-7 cells. The effects of IGF-1 were inhibited by hEAG inhibitors. Moreover, IGF-1 increased mRNA expression of hEAG in a time-dependent manner in parallel with an enhancement of cell proliferation. The MCF-7 cell proliferation induced by IGF-1 is inhibited pharmacologically by Astemizole or Quinidine or more specifically using siRNA against hEAG channel. Either mitogen-activated protein kinase (MAPK) or phosphatidylinositol 3-kinase (PI3K) are known to mediate IGF-1 cell proliferative signals through the activation of extracellular signal-regulated kinase 1/2 (Erk 1/2) and Akt, respectively. In MCF-7 cells, IGF-1 rapidly stimulated Akt phosphorylation, whereas IGF-1 had little stimulating effect on Erk 1/2 which seems to be constitutively activated. The application of wortmannin was found to block the effects of IGF-1 on K<sup>+</sup> current. Moreover, the inhibition of Akt phosphorylation by the application of wortmannin or by a specific reduction of Akt kinase activity reduced the hEAG mRNA levels. Taken together, our results show, for the first time, that IGF-1 increases both the activity and the expression of hEAG channels through an Akt-dependent pathway. Since a hEAG channel is necessary for cell proliferation, its regulation by IGF-1 may thus play an important role in IGF-1 signaling to promote a mitogenic effect in breast cancer cells.

J. Cell. Physiol. 212: 690–701, 2007. © 2007 Wiley-Liss, Inc.

The insulin-like growth factor-1 (IGF-1) plays an important role in the normal development and function of the mammary gland (Hadsell, 2003). However, accumulating evidence suggests that IGF-1 is also involved in breast cancer development (Surmacz et al., 1998). Indeed, elevated levels of circulating IGF-1 are associated with increased risk of breast, prostate, and colon cancer (Hankinson et al., 1998; Pollak, 2000; Hankinson and Schernhammer, 2003; Ibrahim and Yee, 2004; Fletcher et al., 2005). Furthermore, when IGF-1 is over-expressed in the mammary gland of mice, these animals have increased rates of breast cancer development (Hadsell et al., 1996). IGF-1 is a potent mitogenic agent in MCF-7 human breast carcinoma cells (Dufourny et al., 1997; Dupont et al., 2000). The proliferative effect of IGF-1 is mediated by the IGF-1 receptor (Dupont et al., 2000). The enhancing of IGF-1 signaling pathways, by an over-expression of IGF-1 receptors, is involved in breast tissue tumorigenesis (Surmacz, 2000). On the cellular level, it has now been clearly demonstrated that IGF-1 exerts its marked mitogenic effects on breast cancer cells by regulating cell cycle machinery (Van der Burg et al., 1988). Indeed, IGF-1 stimulates cell proliferation by initiating G1 progression to the S phase of the cell cycle (Dufourny et al., 1997). IGF-1 activates two main signaling cascades, the mitogen-activated protein kinase (MAPK) (Skolnik et al., 1993) and the phosphatidylinositol

3-kinase (PI3K) pathways (Backer et al., 1992). Studies on the MCF-7 breast cancer cell line have revealed that the PI3K/Akt pathway, but not the MAPK cascade, is crucial in the cell cycle progression induced by IGF-1 (Dufourny et al., 1997).

Potassium (K<sup>+</sup>) channel activity is known to be linked to cell proliferation and cell cycle progression in various cell types, including MCF-7 cells (Wonderlin and Strobl, 1996; Ouadid-Ahidouch et al., 2001; Pardo et al., 2005). This is supported by the finding that K<sup>+</sup> channel blockers inhibit cell proliferation,

Contract grant sponsor: Ministère de l'Éducation Nationale, de la Recherche et de la Technologie (MENRT).

Contract grant sponsor: Association pour la Recherche sur le Cancer (ARC).

\*Correspondence to: Halima Ouadid-Ahidouch, Laboratoire de Physiologie Cellulaire et Moléculaire, Faculté des Sciences, 33 Rue St. Leu, 80039 Amiens, France. E-mail: ha-sciences@u-picardie.fr

Received 30 March 2006; Revised 26 January 2007; Accepted 29 January 2007

DOI: 10.1002/jcp.21065

thereby leading to membrane depolarization and an arrest in early G1 phase (Wonderlin and Strobl, 1996; Ouadid-Ahidouch et al., 2001; Wang, 2004). Indeed, there is good evidence from several cell lines that membrane potential in early G1 phase is depolarized, and the progression through G1 into S phase is accompanied by a hyperpolarization of the membrane potential induced by  $K^+$  channels (Wonderlin and Strobl, 1996). In accordance with this,  $K^+$  channel antagonists usually inhibit cell proliferation (Conti, 2004; Guo et al., 2005; O'Grady and Lee, 2005).

Human ether à go-go (hEAG)  $K^+$  channels are reported to have oncogenic properties (Pardo et al., 1999). Their distribution is restricted to the brain in normal tissue, while becoming ubiquitous in tumor cells. Indeed, hEAG is expressed in cervix cancer cells, breast tumors, neuroblastoma, melanoma, soft tissue sarcoma, and in a range of tumor tissues (Meyer et al., 1999; Pardo et al., 1999; Ouadid-Ahidouch et al., 2001; Hemmerlein et al., 2006; Mello de Queiroz et al., 2006). Moreover, hEAG channels have been suggested as being important for tumor cell proliferation. Inhibition of hEAG channel expression by molecular biology using antisense oligonucleotides and siRNA, or pharmacological technology with imipramine, astemizole, or quinidine reduces cell proliferation in cancer cell lines (Pardo et al., 1999; Niemeyer et al., 2001; Ouadid-Ahidouch et al., 2001; Gavrilova-Ruch et al., 2002; Weber et al., 2006).

In previous studies, we reported that hEAG channels play a crucial role in regulating MCF-7 cell cycle progression and proliferation (Ouadid-Ahidouch et al., 2001, 2004). Indeed, the addition of serum increases both hEAG  $K^+$  channel expression and activity, thereby inducing an initial hyperpolarization that permits MCF-7 cells to enter into and progress through the G1 phase. Accordingly, hEAG channel inhibition reduces serum-dependant MCF-7 proliferation by accumulating cells in the early G1 phase (Ouadid-Ahidouch et al., 2004). Mounting evidence now shows that  $K^+$  channels play an important role in the mitogenic signal growth factor in various cell types. Consistently, mitogenic signaling mechanisms up-regulate  $K^+$  channel expression and activity (Xu et al., 1999; Gamper et al., 2002). However, the role of hEAG channels in the IGF-1 mitogenic effect in breast cancer cells is still largely unknown.

The aim of the present study was therefore to (i) determinate and characterize the functional and the transcriptional regulation of hEAG channels by IGF-1 (ii) identify the mechanism by which IGF-1 regulates hEAG  $K^+$  channels, and (iii) establish the involvement of hEAG  $K^+$  channels in IGF-1-mediated MCF-7 proliferation.

The results reported in this study reveal that IGF-1 mitogenic activity in the MCF-7 breast cancer cell line is directly correlated with changes in hEAG  $K^+$  channel activity. Specific blockade hEAG  $K^+$  channels with RNA interference technology or a pharmacological blockade inhibit the proliferative effect of IGF-1. Moreover, application of hEAG  $K^+$  blockers provoked an arrest in the G1 phase, pointing to a role for hEAG  $K^+$  channels in the proliferative action of this growth factor. IGF-1 also increases the hEAG mRNA level, suggesting a transcriptional regulation of these channels by IGF-1. Finally, the inhibition of Akt phosphorylation or a specific reduction of Akt kinase activity, diminish the effect of IGF-1 on  $K^+$  current and reduce the hEAG mRNA level. Taken together, these results show that hEAG  $K^+$  channels appear to be a target of Akt-dependent pathways activated by IGF-1.

## Materials and Methods

### Cell culture and cell synchronization

The MCF-7 breast cancer cell line was obtained from the American Type Culture Collection. MCF-7 cells (between passages 150 and 206)

were grown in Eagle's Minimum Essential Medium (EMEM; Gibco-Invitrogen, Cergy Pontoise, France) supplemented with 5% fetal bovine serum (FBS), L-glutamine (2 mM), and gentamicin (50  $\mu$ g/ml) (Gibco). The culture medium was changed every 2 days. Cells were maintained at 37°C in a humidified atmosphere with 5%  $CO_2$ .

To obtain cells accumulated in the early G1 phase, cells were cultured in EMEM supplemented with 5% FBS and prior to our experiments, cells were incubated for 24 h with serum- and phenol red-free EMEM (Ouadid-Ahidouch et al., 2001, 2004). This environment was used as a control condition in our experiment to study IGF-1 action.

### Cell proliferation assay

MCF-7 cells were grown in 96-well plates at 750 cells/well in EMEM with 5% FBS. To investigate the effect of IGF-1 on cell proliferation, after 72 h cells were pre-incubated in serum- and phenol red-free EMEM for 24 h, then incubated in IGF-1 and drugs were added to the serum- and phenol red-free medium. For control purposes, all inhibitors were applied to the serum- and phenol red-deprived cells in the absence of IGF-1. The medium was changed every day. After 2 days of treatment, the number of living cells was estimated by a colorimetric method using an MTS reagent (Celltiter 96<sup>®</sup> Aqueous Non-Radioactive Cell Proliferation Assay, Promega, Charbonnières, France). The results were expressed as a percentage of living cells in each condition tested and normalized to control conditions. Moreover, we used the Trypan blue exclusion assay to determine the MCF-7 cell rate viability.

### Electrophysiology

For electrophysiological analysis, MCF-7 cells were cultured in 35 mm petri dishes. Electrophysiological signals were recorded, amplified, digitized, and analyzed with the use of an Axopatch 200B patch-clamp (Axon Instruments, Burlingame, CA) in conjunction with Labmaster hardware (Digitdata I 200, Axon Instruments) and Pclamp software (ver 6.03, Axon Instruments). The whole-cell mode of the patch-clamp technique was used with 4–7 M $\Omega$  resistance borosilicate fire-polished pipettes (Hirschmann<sup>®</sup>, Laborgerate, Eberstadt, Germany). Seal resistance was typically in the 10–20 G $\Omega$  range. After formation of a seal, the amplifier was switched to voltage-clamp mode and currents attained stable values within 3–5 min. All recordings were made without leak subtraction. Results were expressed using current-densities (pA/pF) instead of current amplitude. The cell surface of the MCF-7 cells was thus estimated by measuring their membrane capacitance ( $20.8 \pm 4.7$  pF,  $n = 63$ ). Whole-cell current was elicited by voltage ramp or by voltage step from  $-80$  to  $+80$  mV delivered at 30 sec intervals for 250 msec, applied from a holding potential of  $-40$  mV. The cell under investigation was continuously superfused with control or test solutions. All electrophysiological recordings were performed at room temperature.

### Solution

Before recording, the culture medium was replaced with a bath of extracellular solution containing (in mM): NaCl 145, KCl 5,  $CaCl_2$  2,  $MgCl_2$  1, HEPES 10, glucose 5 at pH 7.4 (NaOH). Patch pipettes were filled with an intracellular solution containing (in mM): KCl 150,  $MgCl_2$  2, HEPES 10, EGTA 1.1 at pH 7.2 (KOH).

### RNA extraction and reverse transcription-polymerase chain reaction (RT-PCR)

Total RNA was extracted from approximately  $1 \times 10^6$  cultured cells using the Trizol method (Invitrogen, Cergy Pontoise, France) according to the manufacturer's instructions. RNA samples were treated with 1 U of DNase I (Promega, France) at 37°C for 30 min. A phenol/chloroform (vol/vol) extraction was performed and RNA was precipitated with ethanol and then dissolved in 20  $\mu$ l of sterile distilled water. The RNA level was measured by spectrophotometry (OD at 260 nm). For each condition, the same amount of RNA was reverse-transcribed into cDNA using an SSII kit (Invitrogen) following the manufacturer's instructions. Complementary DNA was stored at  $-20^\circ C$ . The PCR primers used to amplify the RT-generated hEAG cDNAs were designed on the basis of established GenBank sequences. The primers for hEAG cDNA were: 5'-CGCATGAACACTCTGAAGACG-3' (nucleotides 898–918,

GenBank accession AF078741 and AF078742) and 5'-TCTGTGGATGGGGCGATGTC-3' (nucleotides 1376–1355). The expected amplified DNA length is 479 bp for hEAGa and 560 bp for hEAGb as described by Ouadid-Ahidouch et al. (2001). Primers were synthesized by Invitrogen. PCR was performed on the RT-generated cDNA using an Applied Biosystems GeneAmp 2700 PCR system cyclor. PCR reaction mixtures contained 1  $\mu$ l cDNA, 1  $\mu$ l of dNTPs (10 mM; Invitrogen), 2.5  $\mu$ l of sense and antisense primer (both 5  $\mu$ M), 0.2  $\mu$ l of Taq DNA polymerase (1 U) (Invitrogen), 5  $\mu$ l of PCR buffer and 1.5  $\mu$ l of MgCl<sub>2</sub> (50 mM) in a final volume of 50  $\mu$ l. Samples were first incubated for 2 min at 94°C, followed by 34 cycles of 30 sec at 95°C, 30 sec at 58°C, and 40 sec at 72°C, followed by a final extension at 72°C for 7 min. PCR products (10  $\mu$ l) were analyzed by electrophoresis in a 1.3% agarose gel in 0.5  $\times$  TBE and stained with ethidium bromide. To assess the relative changes in hEAG mRNA content by IGF-I treatment, semi-quantitative RT-PCR was performed using  $\beta$ -actin as an internal standard. The following primers were used to amplify a 210 bp of fragment  $\beta$ -actin cDNA: 5'-CAGAGCAAGA-GAGGCATCCT-3' and 5'-GTTGAAGGTCTCAAACATGATC-3'. The PCR conditions were the same as above, except for 25 cycles. The reaction products were separated by electrophoresis in 1.3% agarose gel in 0.5  $\times$  TBE and stained with ethidium bromide. The PCR products were quantified using Quantity One software (Biorad, Marnes La Coquette, France). The final normalized results were calculated by dividing the image density of the hEAG PCR product by the density of the amplified  $\beta$ -actin product.

#### Western blotting analysis

Serum- and phenol red-deprived MCF-7 cells were pre-incubated for 30 min with various PI3K and MAPK inhibitors, then treated with IGF-I (20 ng/ml) at the indicated time. The cells were washed twice in the phosphate-buffered saline (PBS), lysed in Laemmli's buffer (Tris-base 62.5 mM pH 6.8, glycerol 10%, 2- $\beta$  mercaptoethanol 5%, SDS 2.3%, and 0.025% of bromophenol blue) and heated thrice to 95–100°C for 10 min.

Phosphorylation of Akt and Erk1/2 proteins was detected by Western blotting. Cell lysates were separated by electrophoresis on SDS-PAGE and blotted onto nitrocellulose membrane. Blots were incubated with the following antibodies: anti-phospho-Akt<sup>ser473</sup> antibody (Cell Signalling Technology, Bonton) or anti-Akt (Santa Cruz Biotechnology, CA), anti-phospho-Erk1/2 antibody or anti-Erk1/2 antibody (Cell Signaling Technology), overnight at 4°C in Tris-buffered saline buffer containing Tween-20 (0.2%) (TBS-T). Membranes were washed three times in TBS-T and then incubated with horseradish peroxidase-conjugated secondary antibody for 1 h at room temperature. After three washes in TBS-T, the immuno-reactive bands were detected using the ECL chemiluminescent system (Amersham-Biotech, Sunnyvale, CA).

#### Purification of TAT-Akt fusion proteins

Purification of TAT fusion proteins was performed as described by Krosil et al. (2003) with the following modifications: BL21 (DE3) pLysS bacteria (Stratagene, Amsterdam, Netherlands) expressing the TAT-Akt fusion proteins were cultured in LB broth medium containing 50  $\mu$ g/ml Ampicillin and 34  $\mu$ g/ml Chloramphenicol at 37°C. Protein expression was induced by the addition of 1 mM IPTG at 37°C for 4 h. Cells were harvested and sonicated in buffer A (8 M urea, 20 mM HEPES (pH = 8.0), and 500 mM NaCl). Lysates were clarified by centrifugation at 13,200 rpm for 4 min at 4°C. The supernatants containing the recombinant TAT-Akt fusion proteins were equilibrated in 30 mM Imidazole and then applied to Ni-NTa Agarose columns (Qiagen, Courtaboeuf, France). Columns were washed with six bed volumes of buffer B (4 M urea, 20 mM HEPES (pH = 8.0), 500 mM NaCl and 30 mM Imidazole). After washing, bound proteins were eluted with buffer B containing 250 mM Imidazole. Eluates containing the purified proteins were dialyzed against PBS with four overnight buffer changes at 4°C. The purity of TAT-Akt fusion proteins was assessed by coomassie blue stained SDS-PAGE and the concentration of TAT fusion proteins was assessed using standard BSA concentrations.

#### In vitro studies of TAT-Akt fusion proteins

MCF-7 cells were cultured in 35 mm petri dishes at a density of  $2.5 \times 10^5$  cells in EMEM with 5% FBS. After 24 h, the cells were pre-incubated in serum- and phenol red-free EMEM for 24 h with the

various TAT-Akt fusion proteins. Then cells were re-incubated with TAT-Akt fusion proteins and stimulated with IGF-I (20 ng/ml) for 16 h. Cells were then prepared for RT-PCR studies and the transduction efficiency of TAT-Akt fusion proteins in these cells was evaluated by Western blotting using anti-HA (Roche, Neuilly Sur Seine, France) and anti-Akt (Cell Signalling Technology) antibodies.

#### Cell cycle analysis

MCF-7 cells were grown in EMEM with 5% FBS. After 72 h, cells were pre-incubated in serum- and phenol red-free EMEM for 24 h, then incubated in IGF-I with or without drugs for 48 h. Cell cycle analysis was performed by measuring cellular DNA content by flow cytometry. Cells were collected by trypsinization, resuspended in 300  $\mu$ l PBS-EDTA (5 mM) and fixed with 700  $\mu$ l absolute ethanol. After fixation, cells were pelleted by centrifugation, resuspended in PBS-EDTA (5 mM), treated with ribonuclease at a final concentration of 10  $\mu$ g/ml (Sigma, Saint Quentin Fallavier, France) for 30 min and stained with propidium iodide (Sigma) at a final concentration of 50  $\mu$ g/ml. To assess cell cycle distribution patterns (G0/G1, S, and G2/M phases), the stained samples were measured using an elite Beckman/Coulter flow cytometer.

#### siRNA cell transfection

The hEAG siRNA (sihEAG) sequence used was 5'-CUGGACAUGGACCAAGUGGAC(dTdT)-3' (position 1578–1598 on hEAG1a sequence and position 1659–1679 on hEAG1b sequence, GenBank accession AF078741 and AF078742 respectively) as described by Weber et al. (2006). Control experiments were performed either by applying the nucleofection alone (nucleofected cells), or by transfecting a specific siRNA against mouse TRPC6 which had no known target in mammalian genomes (cells nucleofected by control siRNA) 5'-UAUUGCCGAGACCGUUCU(dTdT)-3' (position 1591–1609, GenBank accession MMU49069). MCF-7 cells ( $2 \times 10^6$ ) were transfected with 2  $\mu$ g of siRNA (equivalent to 1.3  $\mu$ M), using a Nucleofector device and corresponding kit (Amaxa, Inc., Cologne, Germany). Transfection protocols were performed following the manufacturer's instructions (program E-014; solution V). Using the nucleofector technique, Gresch et al. (2003) have reported that the nucleofection by 1  $\mu$ M siRNA is efficient, optimal and without any non-specific effects. According to these results, we chose to use sihEAG at 2  $\mu$ g (equivalent to 1.3  $\mu$ M). Immediately after transfection, cells were cultured in EMEM medium with 5% FBS in 60 mm petri dishes at  $2.75 \times 10^5$  cells for PCR study and in 96-well plates at  $7 \times 10^3$  cells for proliferation assay.

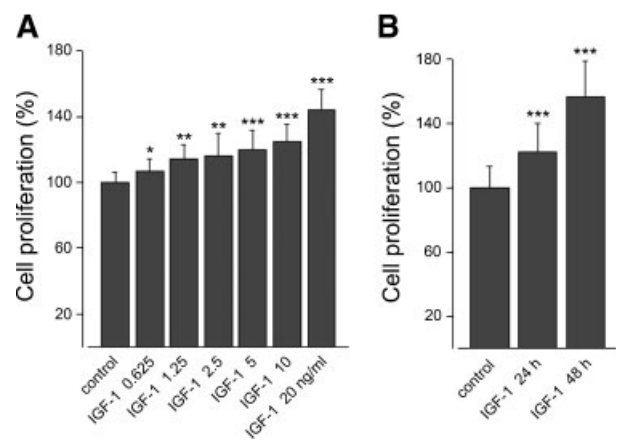


**Fig. 1. IGF-I increases MCF-7 cell proliferation in a concentration and time-dependent manner.** MCF-7 cells were cultured in 96-well plates and then serum- and phenol red-deprived for 24 h. Under these conditions, cells were incubated with the indicated concentrations of IGF-I for 48 h (A) or with 20 ng/ml IGF-I for 24 or 48 h (B). The cell proliferation percentage was determined by a colorimetric method. Values indicated are mean  $\pm$  SE of 16 wells. \*\*\* $P < 0.001$ , \*\* $P < 0.01$ , \* $P < 0.05$ .

**RT-PCR for siRNA studies**

RNA extraction conditions remained unchanged from those previously described. Only primers and PCR conditions changed. The primers for hEAG were: 5'-CGCATGAACTACCTGAAGACG-3' (nucleotides 898–918, GenBank accession AF078741 and AF078742) and 5'-AGGGAGCCAGAAACCACAAAGCAGA-3' (nucleotides 1808–1832 and nucleotides 1889–1913, GenBank accession AF078741 and AF078742 respectively). The amplified PCR product length is 935 bp for hEAG1a and 1016 bp for hEAG1b. The PCR conditions were 5 min at 95°C, followed by 34 cycles of 30 sec at 95°C, 30 sec at 68°C and 1 h 15 min at 72°C, followed by a final 7 min extension at 72°C.

**Drugs and plasmids**

For all experiments, MCF-7 cells were activated with recombinant human IGF-1 (Promocell GmbH, Heidelberg, Germany). For the pharmacological characterization of the IGF-1 sensitive current,

astemizole (AST) and quinidine (Sigma) were added to solutions or to the cell culture medium. To block the IGF-1 signaling pathways, the PI3K inhibitor wortmannin, the MAPK cascade inhibitors UO126 and PD98059 (Sigma) were made in DMSO. The final concentration of DMSO was  $\leq 1/1,000$ .

The coding regions of Akt and Akt ( $K_{179} \rightarrow M$ ) were amplified by PCR and cloned at the NcoI and EcoRI sites of the bacterial expression vector pTAT-HA.

**Statistical analysis**

Data are presented as mean  $\pm$  SE (n = number of individual measurements). The student's *t*-test was used to compare treatment means with control means and to test significant differences. Differences between values were considered significant (\*) when  $P < 0.05$ ; very significant (\*\*) when  $P < 0.01$ , and highly significant (\*\*\*) when  $P < 0.001$ .

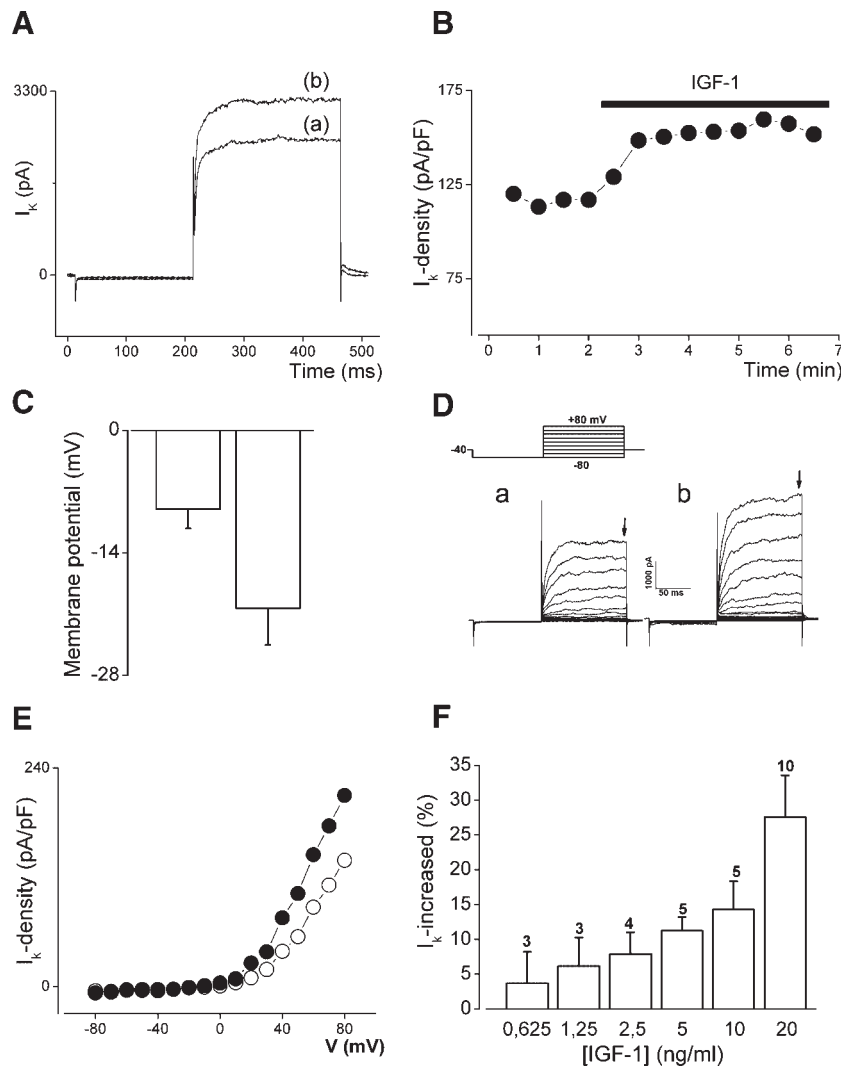


**Fig. 2.** IGF-1 increases  $K^+$  current recorded in serum- and phenol red-deprived MCF-7 cells. **A:** representative  $K^+$  current traces recorded in MCF-7 cells under voltage clamp conditions before (a) and after (b) IGF-1 (20 ng/ml) application on the bath solution. Current was elicited by voltage step from  $-80$  to  $+80$  mV for 250 msec from a holding potential of  $-40$  mV. **B:** The time-course of IGF-1 effect was measured at  $+80$  mV. **C:** The histogram shows the mean values of the hyperpolarization induced by IGF-1 (20 ng/ml) ( $n = 19$ ). **D:**  $K^+$  current was elicited by 10 mV increment from  $-80$  to  $+80$  mV for 250 msec, applied from a holding potential of  $-40$  mV (schematically shown at the top of a and b) and recorded before (a) and after (b) IGF-1 application. **E:**  $I_K$ -density/voltage relationships obtained by measuring the maximal amplitude  $K^+$  current before (open circle) and after (closed circle) the extra-cellular application of IGF-1 (20 ng/ml). **F:** Dose-dependent activation of  $K^+$  current by IGF-1. The columns represent the mean  $\pm$  SE. The number of cells investigated is indicated above each column.

## Results

### IGF-1 induces serum- and phenol red-deprived MCF-7 cell proliferation

Initial studies were carried out to determine the effect of IGF-1 on promoting cell proliferation. To evaluate the mitogenic effect of IGF-1, we used a serum- and phenol red-deprived medium as control condition. Cells were then incubated in serum- and phenol red-deprived for 24 h and treated with IGF-1 for 48 h. Figure 1A shows that IGF-1 increased cell proliferation in a dose-dependent manner. Physiological concentrations of IGF-1 measured in normal breast tissue during the follicular phase of the menstrual cycle (0.625 ng/ml) and during the luteal

phase of the menstrual cycle (1.25 ng/ml) (Dabrosin, 2003) were able to significantly increase MCF-7 cell proliferation by  $6.7 \pm 7.9\%$  ( $n = 15$ ) and  $14.1 \pm 8.9\%$  ( $n = 16$ ) respectively after 48 h of treatment. The maximal increase  $44.3 \pm 12.4\%$  ( $n = 16$ ) was obtained for 20 ng/ml. Because there is no indication about in situ physiological concentrations of IGF-1 in mammary cancer tissue and as 20 ng/ml is the most commonly used concentration as a mitogenic stimulus to study IGF-1 activity on the MCF-7 cell line (Hamelers et al., 2002), we consequently chose to use this concentration in all our experiments. Furthermore, the effect of IGF-1 was time-dependent (Fig. 1B). Indeed, MCF-7 cell proliferation increased by  $22.2 \pm 18.1\%$  ( $n = 15$ ) and  $56.6 \pm 22.1\%$  ( $n = 15$ ) after 24 and 48 h IGF-1

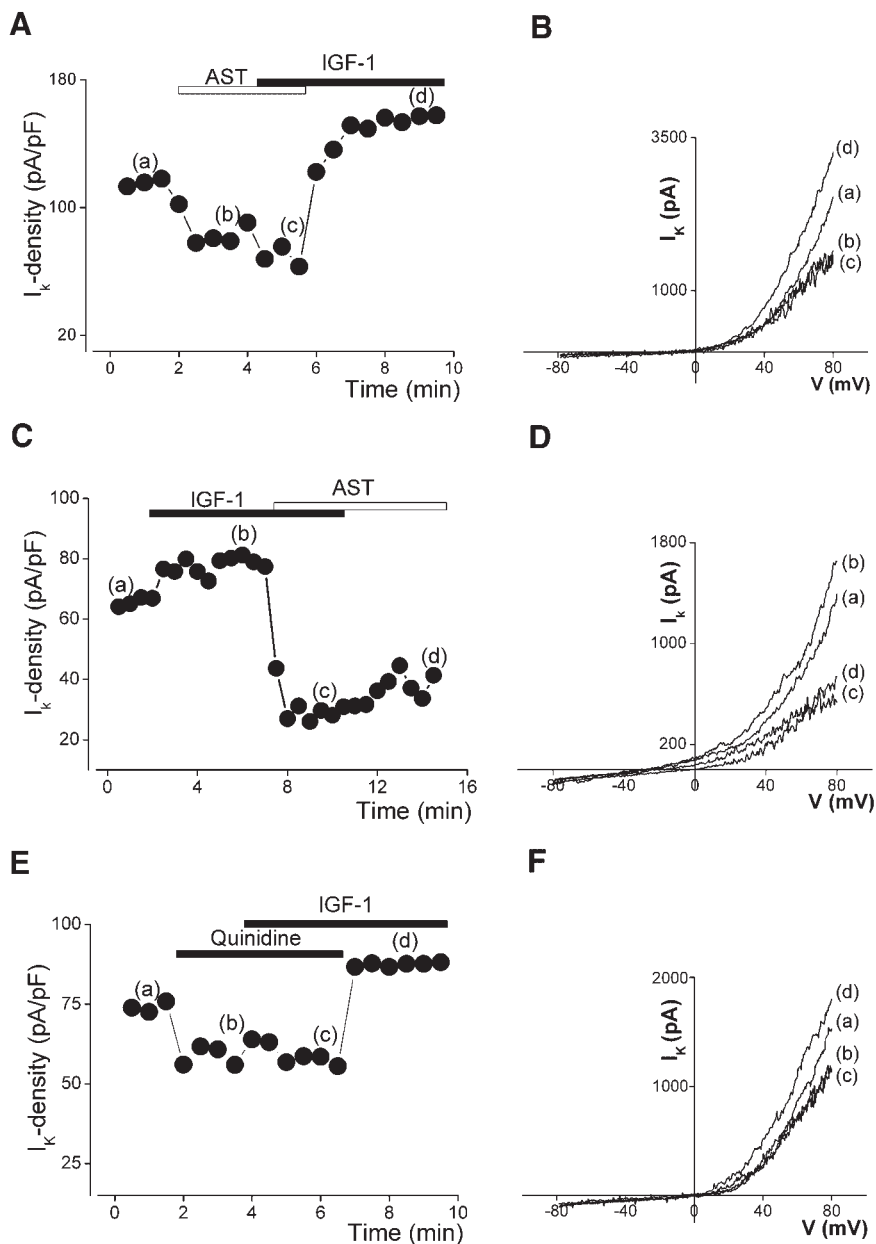


**Fig. 3.** IGF-1 increases hEAG  $K^+$  channel activity in serum- and phenol red-deprived MCF-7 cells. We used a hEAG channel blocker called astemizole (AST) at  $10 \mu\text{M}$ , both to prevent (A,B) and block (C,D) the IGF-1 effect. Quinidine treatment was used to confirm these results (E,F). In all cases,  $K^+$  current was activated by voltage ramp from  $-80$  to  $+80$  mV for 250 msec, applied from a holding potential of  $-40$  mV. Graphs shown on A,C,E represent the time-course of the IGF-1 effect on  $K^+$  current-density (pA/pF) measured at  $+80$  mV, and B,D,F, representative current traces (pA) corresponding to the points indicated.

treatments respectively (Fig. 1B). These results show that IGF-1 leads to MCF-7 cell proliferation, which correlates with those previously reported for the same cells by Van der Burg et al. (1988) and Dufourny et al. (1997).

#### IGF-1 stimulated $K^+$ channel activity

To test a conceivable relationship between IGF-1 and  $K^+$  channel activity, we used the whole cell configuration of the patch-clamp technique.  $K^+$  current was elicited by voltage steps from  $-80$  to  $+80$  mV from a holding potential of  $-40$  mV. To study the effect of IGF-1 on  $K^+$  channel activity in MCF-7 cells, the cells were incubated in serum- and phenol red-free medium for 24 h before their stimulation with IGF-1 (20 ng/ml). Upon

exposure of MCF-7 cells to 20 ng/ml of IGF-1, the amplitude of the  $K^+$  current-density increased markedly (Fig. 2A). The time course showed that the amplitude of the  $K^+$  current-density increased by 29% within 1–2 min after exposure to IGF-1 stimulation (Fig. 2B). The increase in  $K^+$  current-density in MCF-7 cells induced by IGF-1 was accompanied by a 12 mV hyperpolarization of membrane potential of ( $n = 19$ ) (Fig. 2C). The  $K^+$  current-density/voltage relationships recorded before and after IGF-1 application are shown in Figure 2D,E. The application of IGF-1 did not modify the threshold of this activation (Fig. 2E) and the effect observed was dose dependent (Fig. 2F). The physiological IGF-1 concentration measured during the follicular phase (0.625 ng/ml) enhanced the  $K^+$  current-density ( $n = 3$ ), and the maximal  $K^+$  current-density

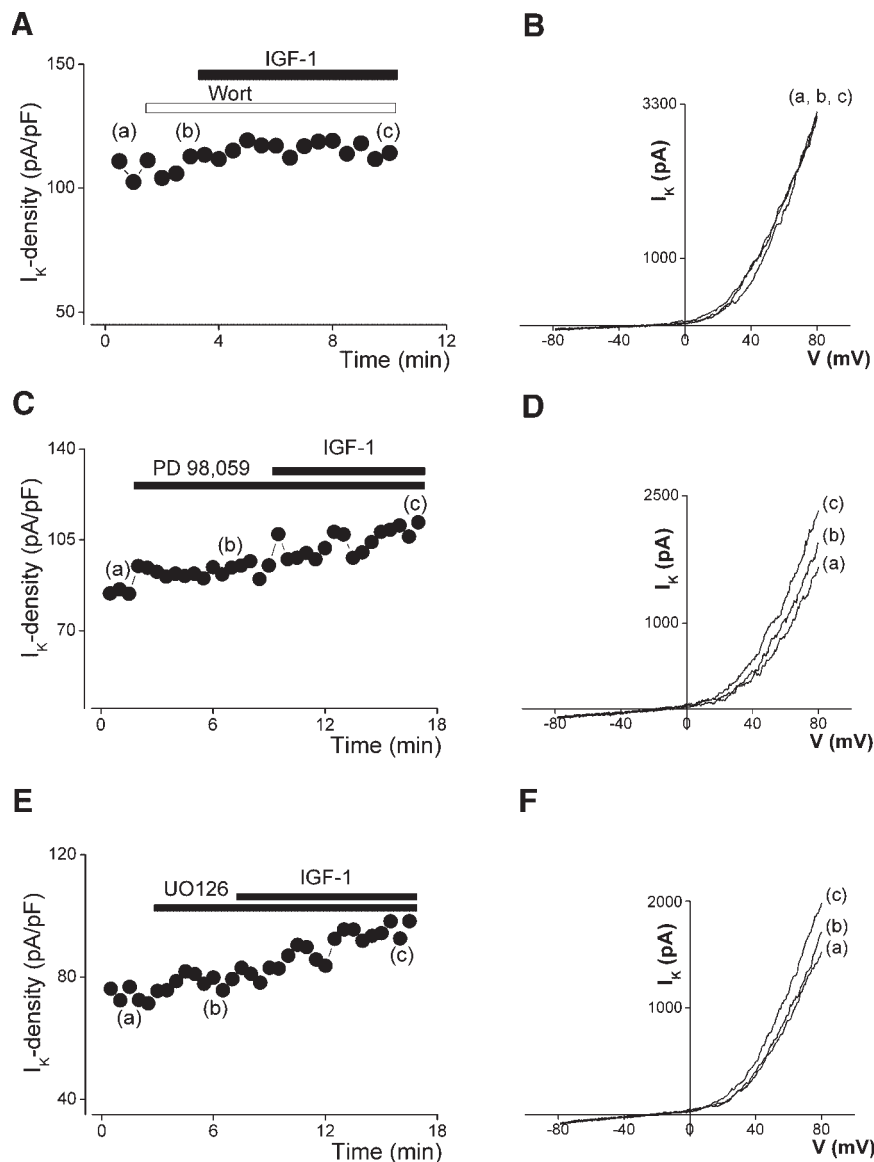


**Fig. 4.** IGF-1 activates hEAG  $K^+$  channel activity through PI3K/Akt. To determine the signaling pathways involved in the regulation of hEAG channel activity by IGF-1, the PI3K inhibitor wortmannin (100 nM) (A,B) and MAPK inhibitors PD98059 (40  $\mu$ M) (C,D), and UO126 (5  $\mu$ M) (E,F) were applied to the bath solution, then the MCF-7 cells were stimulated by IGF-1 (20 ng/ml). In all cases,  $K^+$  current was activated by voltage ramp from  $-80$  to  $+80$  mV for 250 msec, applied from a holding potential of  $-40$  mV. Graphs shown represent the time-course of the IGF-1 effect at  $+80$  mV (left), and representative current traces corresponding to the points indicated (right).

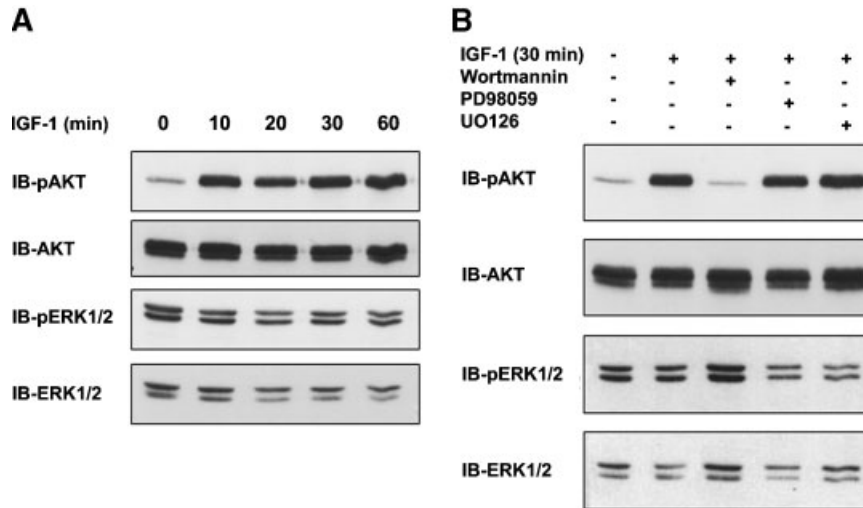


**Fig. 5.** Activation of Akt phosphorylation by IGF-1. Serum- and phenol red-deprived MCF-7 cells were treated with IGF-1 (20 ng/ml) for the times indicated (A), and with or without pre-incubation for 30 min with PI3K inhibitor wortmannin (100 nM) or with inhibitors of MAPK signaling PD98059 (40  $\mu$ M) and UO126 (5  $\mu$ M) (B). Cells were lysed as described under Materials and Methods Section. Western blotting first probed with anti-phospho-<sup>ser473</sup>Akt or with anti-phospho-Erk1/2 were stripped and reprobed with antibodies to the corresponding proteins. Each immunoblot is representative of four similar experiments.

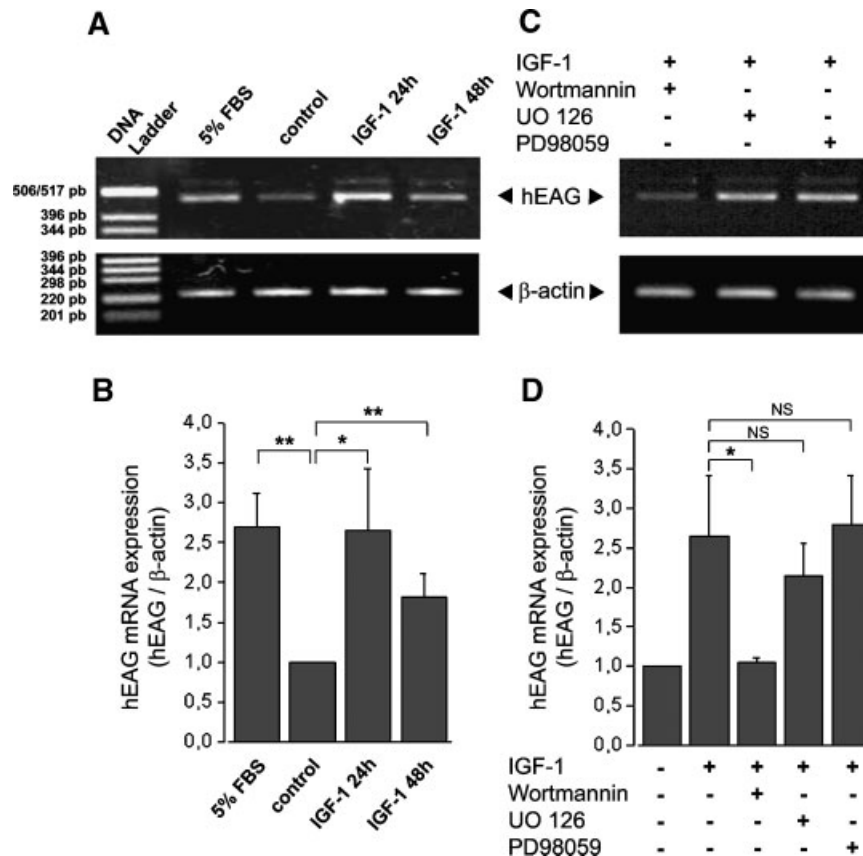


**Fig. 6.** Modulation of hEAG mRNA expression by IGF-1 is dependent on the Akt-dependent pathway. Up-regulation of hEAG mRNA transcripts by IGF-1 on hEAG mRNA expression and the signaling pathway involved in this regulation, MCF-7 cells were serum- and phenol red-deprived for 24 h and then incubated with 20 ng/ml IGF-1 for 24 or 48 h in the presence of IGF-1 alone (A,B) or in the presence of both IGF-1 and inhibitors of PI3K (wortmannin, 100 nM) and MAPK cascade (PD98059, 40  $\mu$ M and UO126, 5  $\mu$ M) (C,D). FBS medium (5%) was used as a positive test. hEAG mRNA levels were quantified and normalized to the amplified  $\beta$ -actin products. Each column represents mean  $\pm$  SE (n = 3). \*\* $P < 0.01$ , \* $P < 0.05$ .

was obtained at 20 ng/ml IGF-1 ( $27.5 \pm 5.9\%$ ,  $n = 10$ ). Taken together, these results indicate that IGF-1 modulates the  $K^+$  channel activity and supports a hyperpolarization of the membrane potential.

#### IGF-1 increased hEAG $K^+$ current-density

We have previously demonstrated that hEAG  $K^+$  channels are preferentially expressed and functional in MCF-7 arrested in the early G1 phase, by starvation during 24 h (Ouadid-Ahidouch et al., 2001, 2004). Under these control conditions, we investigated whether IGF-1 stimulated hEAG  $K^+$  channel activity. We found that astemizole, a specific hEAG channel inhibitor, reduced  $K^+$  current-density by  $21.5 \pm 3\%$  ( $n = 6$ ) and  $36.8 \pm 6.8\%$  ( $n = 7$ ) when used at 5 and 10  $\mu$ M respectively (data not shown). The effect of this blocker was reversible (data not shown). In the presence of 10  $\mu$ M astemizole, IGF-1 failed to increase  $K^+$  current-density (Fig. 3A,B). However, after astemizole removal we noticed an increase in  $K^+$  current of 35.4% from the control by IGF-1 (Fig. 3A,B). Moreover, the IGF-1 effect on  $K^+$  current-density was fully blocked by the addition of 10  $\mu$ M astemizole (Fig. 3C,D,  $n = 5$ ). Similar results were obtained when using quinidine, a well-known hEAG  $K^+$  channel activity blocker (Fig. 3E,F). These results indicate that IGF-1 activates cell-membrane hEAG  $K^+$  channel activity in MCF-7 cells.

#### PI3K/Akt but not MAPK is involved in the IGF-1-dependent hEAG $K^+$ channel activity

The two major routes involved in IGF-1 receptor signaling are the PI3K/Akt and MAPK pathways (Backer et al., 1992; Skolnik et al., 1993). To determine whether IGF-1-induced hEAG channel activity is dependent on PI3K/Akt or MAPK signaling pathways, we used chemical inhibitors of PI3K (wortmannin) and MAPK (PD98059, and UO126). MCF-7 cells were pre-treated with wortmannin, PD98059 or UO126 and then stimulated with IGF-1. Wortmannin completely suppressed the IGF-1-induced increase in  $K^+$  current-density (Fig. 4A,B). In contrast, PD98059 (Fig. 4C,D) and UO126 failed to prevent the IGF-1 effect (Fig. 4E,F). These results suggest that PI3K/Akt participates directly in the IGF-1-induced hEAG  $K^+$  channel activity, whereas the MAPK pathway is not involved in the IGF-1 response. Subsequently, both IGF-1 activation of signaling pathways and the signaling pathways inhibitors' action were studied using Western blotting. As shown in Figure 5A, IGF-1 induced a strong Akt phosphorylation after a 10 min treatment and persisted for 60 min. Pre-incubation with wortmannin for 30 min totally abolished IGF-1 stimulated Akt phosphorylation (Fig. 5B). In contrast, Erk1/2 phosphorylation was weakly activated by IGF-1 stimulation (Fig. 5A,B). Pre-treatment with PD98059 and UO126 reduced Erk1/2 phosphorylation (Fig. 5B). These data confirm that, in MCF-7 cells, IGF-1 activates the PI3K/Akt pathway, which is essential for IGF-1 increased hEAG  $K^+$  channel activity. Furthermore, the MAPK cascade seems to be activated constitutively.

#### IGF-1 increased hEAG mRNA levels through the Akt-dependent pathway

It has been shown that IGF-1 is also able to produce a transcriptional regulation of numerous ionic channels in normal and pathological situations (Guo et al., 1998; Shen et al., 2004). In this context, we also examined whether IGF-1 stimulates hEAG channel expression. Semi-quantitative RT-PCR data show that IGF-1 stimulated mRNA levels of hEAG in a time-dependent manner (Fig. 6). After 24 and 48 h exposures to IGF-1, hEAG mRNA levels increased significantly, by approximately

threefold and twofold respectively, above control levels (Fig. 6A,B). Next, we investigated the possible contribution of the Erk1/2 and PI3K/Akt pathways to IGF-1 stimulation of hEAG mRNA levels. Treatment with wortmannin totally abolished IGF-1 stimulated hEAG mRNA levels (Fig. 6C,D). In contrast, both PD98059 and UO126 failed to decrease hEAG mRNA levels (Fig. 6C,D). To evaluate in a more definitive

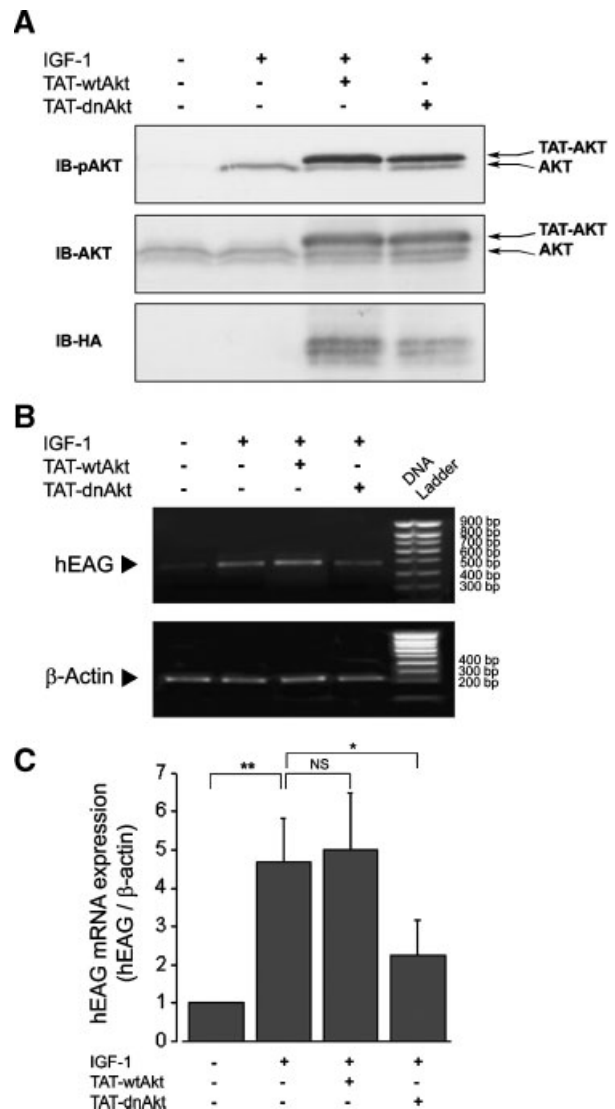


**Fig. 7. Dominant negative Akt reproduces the wortmannin effect: evidence of Akt involvement in regulation of hEAG mRNA expression by IGF-1.** MCF-7 cells were incubated with serum- and phenol red-free medium containing functional TAT proteins fused to the wild-type (TAT-wtAkt) or to a dominant negative form (TAT-dnAkt) of Akt for 30 min (A) and for 24 h (B,C). Then, cells were maintained for 30 min (A) and for 16 h (B,C) in the presence of IGF-1 (20 ng/ml). **A:** Western blot was used to verify the presence of the TAT-Akt fusion proteins (TAT-wtAkt and TAT-dnAkt) in MCF-7 cells. Thus, cell lysates were prepared to detect TAT-Akt proteins by using anti-p<sup>Ser473</sup>-Akt, Akt and HA antibodies. **B:** The transduction of functional TAT proteins fused to the wild-type or to the dominant negative form of Akt in MCF-7 was used to confirm the involvement of Akt-dependent signaling in the regulation of hEAG mRNA expression by IGF-1. After the culture conditions described above, cells were prepared for RT-PCR studies. **C:** hEAG mRNA levels were quantified and normalized to the amplified  $\beta$ -actin products. Each column represents mean  $\pm$  SE ( $n = 3$ ). \*\* $P < 0.01$  and \* $P < 0.05$ .

manner, the crucial importance of the Akt-dependent signaling pathway for IGF-1 stimulated hEAG mRNA levels, we produced and used TAT-Akt fusion proteins that have previously been described (Harir et al., 2007). The use of TAT-fusion proteins is an appealing approach to transducing various types of cells, as they can be delivered very quickly and efficiently to either cell lines or primary cells, simply by adding them to the culture medium (Vocero-Akbani et al., 2001; Krosal et al., 2003). To analyze the role of Akt, we used a TAT-wtAkt (wild-type) and a TAT-dnAkt (dominant negative) fusion protein. The dnAkt form containing the point mutation K179M, that inactivates its kinase activity, has previously been shown to act as a dominant negative mutant by competing with endogenous wtAkt for the binding of the downstream substrates. Accordingly, it was shown, recently, in hematopoietic cells that transduction of TAT-dnAkt, but not TAT-wtAkt proteins, inhibited the phosphorylation of Akt kinase substrates like the Forkhead transcription factors (Franke et al., 1995; Harir et al., 2007). Both TAT-Akt fusion proteins were applied to serum- and phenol red-deprived MCF-7 cells. After 24 h, cells were stimulated by IGF-1 for 16 h. Transduction efficiency of TAT-Akt fusion proteins in MCF-7 cells was evaluated by Western blotting with anti-HA and anti-Akt antibodies (Fig. 7A). Phosphorylation of endogenous Akt and TAT-Akt fusion proteins by IGF-1 stimulation was confirmed with anti-P<sup>Ser473</sup> Akt antibody (Fig. 7A). Using semi-quantitative RT-PCR, we found that TATdn-Akt, but not TAT-wtAkt protein inhibited IGF-1-induced hEAG mRNA expression (Fig. 7B,C). Collectively, these results indicate that modulation of hEAG channel expression by IGF-1 requires the activation of the Akt-dependent pathway.

#### Involvement of hEAG K<sup>+</sup> channel in IGF-1-induced MCF-7 cell proliferation

To determine whether the inhibition of hEAG channel activity would suppress MCF-7 cell proliferation induced by IGF-1, the two hEAG channel blockers, astemizole and quinidine, were added to the cell culture medium. Astemizole inhibited cell proliferation induced by IGF-1 in a concentration-dependent manner ( $n = 19$ ) (Fig. 8A). Astemizole (10  $\mu$ M) inhibited MCF-7

cell proliferation induced by IGF-1 by 61%. When used alone, astemizole had no effect (Fig. 8A). In the same manner, we found that the commonly used concentration of quinidine (20  $\mu$ M) to totally block hEAG channels, significantly reduced the mitogenic action of IGF-1 by 68% ( $n = 20$ ) (Fig. 8B). Furthermore, to determine whether the inhibition of IGF-1 proliferation induced by astemizole and quinidine was accompanied by cell arrest in a specific cell cycle phase, we used flow cytometry to analyze the cell cycle status of MCF-7 cells incubated in IGF-1 alone or with hEAG K<sup>+</sup> channel blockers. After 24 h of serum- and phenol red-deprivation, cells were incubated in IGF-1 (20 ng/ml) in the presence or absence of hEAG K<sup>+</sup> channel blockers for 48 h. Cells incubated in IGF-1 for 48 h showed a distribution with  $71.4 \pm 3.3\%$ ,  $20 \pm 3.2\%$ , and  $8.6 \pm 1.3\%$  in G0/G1, S, and G2/M phases respectively ( $n = 3$ ) (Fig. 8C). Astemizole (5 and 10  $\mu$ M) induced an accumulation of cells in G0/G1 ( $89.2 \pm 2\%$  for 5  $\mu$ M and  $87 \pm 1.55\%$  for 10  $\mu$ M,  $n = 3$ ) and a reduction in the number of cells in the S phase ( $8.6 \pm 1.7\%$ ,  $9.2 \pm 1.3\%$ ) and the G2/M phase ( $2.2 \pm 0.4\%$ ,  $3.8 \pm 0.35\%$ ). Similar results are obtained in the presence of quinidine 20  $\mu$ M (Fig. 8C). Moreover, the Trypan blue exclusion assay showed that MCF-7 cell viability was affected neither by astemizole (5 and 10  $\mu$ M) nor by quinidine (20  $\mu$ M). Taken together, these results show that suppression of hEAG K<sup>+</sup> channel activity inhibited IGF-1 stimulated MCF-7 proliferation by inducing G1 arrest.

To confirm that hEAG K<sup>+</sup> channel activity is required for IGF-1 cell proliferation increase, we used siRNA technology to down-regulate hEAG expression in MCF-7 cells. Cells were transfected using the Nucleofector Technology. The transfection with 2  $\mu$ g of control siRNA did not modify the rate of cell viability compared to nucleofected cells ( $n = 3$ ). A non-significant effect on cell proliferation was also observed between nucleofected cells and cells nucleofected with control siRNA (Fig. 9A). As predicted, IGF-1 incubation for 48 h induced an increase in cell proliferation (Fig. 9A). In contrast, it failed to increase MCF-7 cell proliferation in cells transfected with sihEAG (Fig. 9B). Moreover, transfection with sihEAG reduced cell proliferation by  $33 \pm 3.1\%$  ( $n = 3$ ) compared to control siRNA (Fig. 9B). Taken together, these results demonstrate that hEAG K<sup>+</sup>

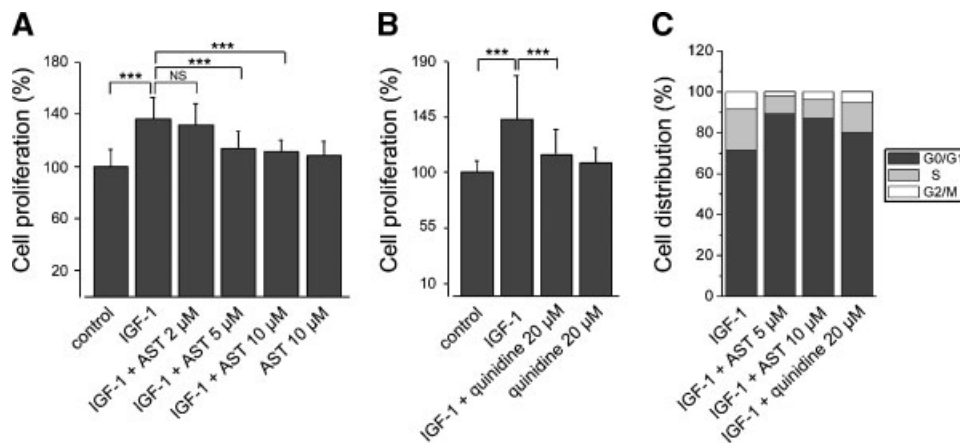


**Fig. 8.** hEAG K<sup>+</sup> channel blockers inhibited cell proliferation induced by IGF-1 and accumulated cells in the G1 phase. **A,B:** hEAG K<sup>+</sup> channel blockers inhibited IGF-1 proliferation. MCF-7 cells were cultured in 96-well plates and then serum- and phenol red-deprived for 24 h. Under these conditions, cells were incubated with 20 ng/ml IGF-1 in the absence or presence of the hEAG channel inhibitors AST at 2  $\mu$ M, 5  $\mu$ M, and 10  $\mu$ M (A) or quinidine at 20  $\mu$ M (B) for 48 h. In order to provide a control sample, all K<sup>+</sup> channels inhibitors were applied alone to the serum- and phenol red-deprived cells. The cell proliferation percentage was determined by a colorimetric method. Values indicated are mean  $\pm$  SE of 20 wells. \*\*\* $P < 0.001$ . **C:** hEAG K<sup>+</sup> channel blockers accumulated cells in the G1 phase. MCF-7 cells were serum- and phenol red-deprived for 24 h, cells were treated with IGF-1 (20 ng/ml) in the absence or presence of AST at 5 and 10  $\mu$ M and quinidine (20  $\mu$ M) for 48 h. Thereafter, cells were collected by trypsinization, stained with propidium iodide and the DNA content was measured by flow cytometry.

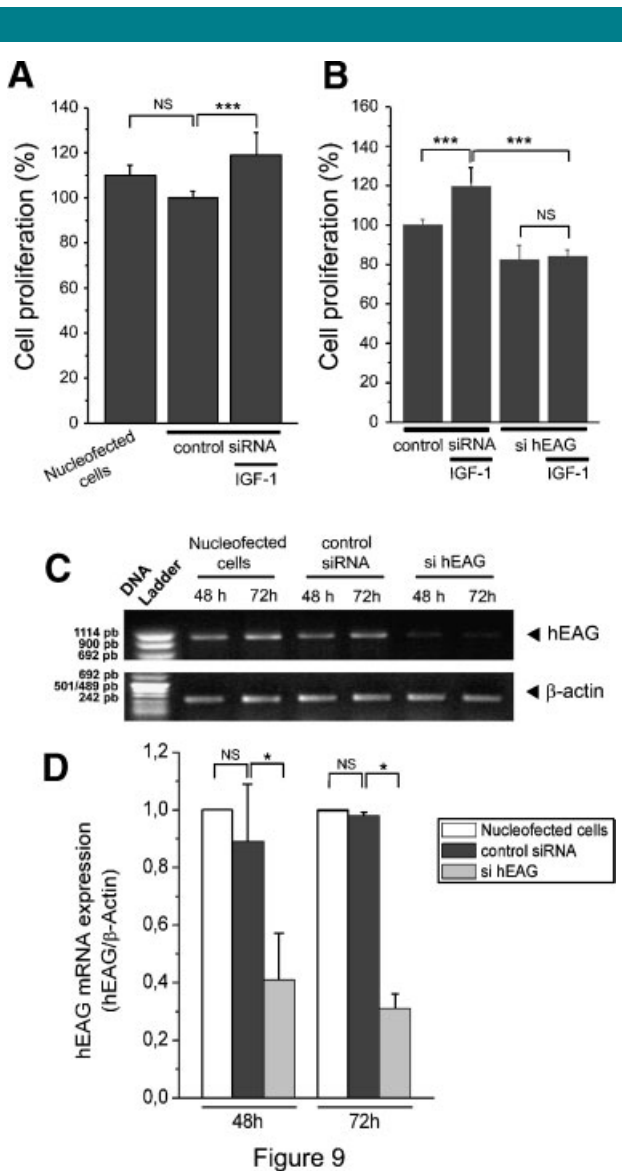


**Fig. 9.** A specific down-regulation of hEAG with siRNA inhibited the IGF-1 proliferative effect. MCF-7 cells were transfected by a Nucleofector device without siRNA (nucleofected cells) and with control siRNA<sub>TRPMouse</sub> (control siRNA) or hEAG siRNA (sihEAG). Then, cells were cultured in EMEM medium with 5% FBS. After 18 h, cells were serum- and phenol red-deprived for 6 h and then incubated with IGF-1 (20 ng/ml) for 24 or 48 h. **A,B:** For proliferation assay, cells were grown in 96-well plates. After 48 h of IGF-1 incubation, cell proliferation was determined by a colorimetric method. IGF-1 was unable to increase cell proliferation in cells transfected by the specific RNAi of hEAG (**B**) compared with cells transfected by control siRNA (**A**). Indicated values are mean  $\pm$  SE of eight wells. Experiments were repeated three times,  $***P < 0.001$ . **C:** Original gels showing reduced mRNA level of hEAG with the corresponding specific RNAi, compared with control RNAi 48 and 72 h after transfection. **D:** hEAG mRNA levels were quantified and normalized to the amplified  $\beta$ -actin products. Each column represents mean  $\pm$  SE ( $n = 3$ ).  $*P < 0.05$ .

channels are strongly involved in MCF-7 cell proliferation induced by IGF-1.

Using semi-quantitative RT-PCR, we demonstrated that sihEAG greatly reduced the hEAG mRNA level. Indeed, compared to cells transfected with control siRNA, cells transfected with sihEAG showed  $50 \pm 0.01\%$  and  $72.5 \pm 0.04\%$

reductions in their hEAG mRNA levels 48 and 72 h after transfection (Fig. 9C,D).

## Discussion

IGF-1 promotes the proliferation, survival, motility, and metastasis of cancer cells (Surmacz, 2000). The role of IGF-1 in regulating cell proliferation by inducing cyclin up-regulation has been well-defined. However, the role of  $K^+$  channels in the mitogenic effect of IGF-1 in breast cancer is as yet incompletely understood. In the present study, we show, for the first time, that hEAG  $K^+$  channel activity is necessary for IGF-1-dependent proliferation and that IGF-1 is able to modulate this hEAG channel activity and expression by the Akt-dependent pathways. This conclusion is supported by the following findings: (1) IGF-1 stimulated cellular proliferation in a concentration-dependent manner. This activity was almost completely blocked by hEAG pharmacological blockers. Moreover, the specific siRNA targeted to hEAG, down-regulated the corresponding genes and inhibited cell proliferation induced by IGF-1, (2) IGF-1 directly up-regulated hEAG channel activity through the Akt-dependent pathway, (3) IGF-1 also increased hEAG mRNA levels, and (4) dominant negative Akt reduced the mRNA levels of hEAG.

Four  $K^+$  channels, including hEAG channels, have been identified as being the main contributors to the  $K^+$  conductance in breast cancer cells (Ouadid-Ahidouch et al., 2001, 2004). The oncogenic potential of hEAG channels (Pardo et al., 1999) and the fact that this channel is used as a marker of cancer development (Farias et al., 2004; Mello de Queiroz et al., 2006; Hemmerlein et al., 2006) lead us to study the relationship between IGF-1 and hEAG channel activity. Moreover, it has been demonstrated that hEAG channel blockers inhibit MCF-7 cell proliferation induced by serum and accumulated MCF-7 cells in the early G1 phase, thereby indicating that this type of  $K^+$  channels plays a critical regulatory role in the growth of human breast cancer cells (Ouadid-Ahidouch et al., 2001, 2004). In this study, we have demonstrated that a shorter application of IGF-1 stimulated hEAG channel activity in a dose-dependent manner. This effect occurs within 1–2 min after IGF-1 exposure, suggesting a direct phosphorylation of the channels, their auxiliary subunits, and/or stimulation of channel trafficking. Up to now, no studies have shown that a short application with IGF-1 is able to modulate ionic channel activity. In fact, it has been only demonstrated that longer incubations with IGF-1 up-regulated  $K^+$  channels activity by a transcriptional effect within 4–6 h (Gamper et al., 2002). Other studies have clearly reported an over-expression of ionic transporters due to IGF-1, including skeletal L-type  $Ca^{2+}$  channels (Zheng et al., 2004),  $Ca^{2+}$  channel  $\alpha_2\delta$ -subunits from rat atria (Chu and Best, 2003) and KCl transporters (Shen et al., 2004). In the present study, we also show a transcriptional effect of IGF-1 on hEAG channels. Indeed, our molecular biology results clearly show that IGF-1 is able to increase hEAG mRNA levels after 24 h incubation.

In breast cancer cells, IGF-1 was shown to induce its mitogenic effect mainly through the PI3K/Akt signaling pathway (Dufourny et al., 1997). In our study, immunoblot analysis in MCF-7 cells revealed an activation of Akt by IGF-1. The time course of Akt phosphorylation shows a maximal activation after 10 min incubation with IGF-1. This result is in accordance with those found by Dufourny et al. (1997) in MCF-7 cells.

Using electrophysiological techniques, it has been shown that IGF-1 mainly regulates the  $K^+$  channel activity by two principal signaling pathways, namely PI3K and MAPK (Gamper et al., 2002; Wei et al., 2004). Wei et al. (2004) have reported that the stimulatory effect of IGF-1 on the apical 70 pS  $K^+$  channel is mediated by a MAPK-dependent pathway. In contrast, the effect of IGF-1 on Kv channels is mediated by PI3K stimulation

(Gamper et al., 2002). Our electrophysiological results in Figure 4 show that the hEAG enhancing activity by IGF-I is inhibited by the addition of wortmannin. Although the specificity of the PI3K inhibitor wortmannin remains questionable, many studies have reported in MCF-7 cells that (i) wortmannin used until 250 nM reduces both the activity of the PI3K and the cell proliferation induced by the IGF-I (Jackson et al., 1998), and (ii) the IGF-I mitogenic effect is induced via PI3K/Akt-dependent pathway (Laban et al., 2003; Dufourny et al., 1997). According to these results, we can suggest that the increase of hEAG expression by IGF-I is mediated by the PI3K/Akt pathway. Moreover, the time course of the IGF-I effect (about 1 min) suggests that the modification of hEAG channel activity is supported by a functional modification such as phosphorylation rather than by transcriptional changes. In our opinion, these effects are more likely to be attributable to an increase in functional channel numbers. Nevertheless, during our electrophysiological studies, we observed that the application of MAPK inhibitors such as UO126 and PD98059 can produce a marginal amplitude increase in hEAG current. We suggest that UO126 and PD98059, in this case, block a constitutive activation of the MAPK pathway. Indeed, a constitutive activation of MAPK is supported by our results (Fig. 5). We can also suggest that this constitutive activation supports a tonic inhibition of the  $K^+$  channels.

Longer applications (about 24 h) of IGF-I produce an increase in hEAG mRNA levels. The hEAG mRNA levels induced by IGF-I were markedly reduced when Akt phosphorylation was inhibited. Most importantly, specific reduction of Akt kinase activity using the dominant negative form of Akt abolished IGF-I stimulated hEAG mRNA levels. Moreover, our results show that the MAPK pathway is little involved in these IGF-I regulated mitogenic processes and is basally active in these cells. Accordingly, IGF-I-treatment results in only slight activation of this pathway.

IGF-I has been demonstrated to play an important role in the regulation of cell proliferation (Jones and Clemmons, 1995). In addition, IGF-I has been shown to induce proliferation of HEK cells through an activation of the  $Kv K^+$  channel family (Gamper et al., 2002). Our results show that treatment of MCF-7 by hEAG channel inhibitors, astemizole and quinidine, inhibit the IGF-I mitogenic effect in a concentration-dependent manner and induce an accumulation of cells in the G1 phase. Unfortunately, specificity of hEAG  $K^+$  channel blockers is largely discussed today. To overcome this problem, we used RNA interference, which represents a suitable alternative to functional blocker of channel activity (Weber et al., 2006; Gurney and Hunter, 2005). siRNA for hEAG has been characterized and does not induce non-specific responses (Weber et al., 2006). sihEAG treatment resulted in a reduction in cell proliferation increase induced by IGF-I (Fig. 9) to an extent comparable to that induced by astemizole and quinidine.

In conclusion, we suggest that IGF-I stimulates cell proliferation by two mechanisms: (i) increasing hEAG  $K^+$  channel activity by a phosphorylation pathway and (ii) increasing the number of hEAG functional channels by up-regulating their mRNA level. These two mechanisms are directly linked to Akt activity. Furthermore, we can also suggest that the predictive status of IGF-I in breast cancer development could be supported by its ability to up-regulate oncogenes expression as hEAG  $K^+$  channels. Blocking hEAG channel activity or expression may provide novel strategies for the reduction of IGF-I-dependent cellular proliferation of breast cancer cells.

### Acknowledgments

Financial support was received from the Association pour la Recherche sur le Cancer (ARC), The Ligue contre le Cancer and the Picardie Region. We wish to thank Dr Valérie

Gouilleux-Gruart for helpful discussions and suggestions on flow cytometry technique. We thank also, Jean François Lefebvre for his excellent technical assistance.

### Literature Cited

- Backer JM, Myers MG, Jr., Shoelson SE, Chin DJ, Sun XJ, Miralpeix M, Hu P, Margolis B, Skolnik EY, Schlessinger J. 1992. Phosphatidylinositol 3'-kinase is activated by association with IRS-1 during insulin stimulation. *EMBO J* 11:3469–3479.
- Chu PJ, Best PM. 2003. Molecular cloning of calcium channel  $\alpha(2)\delta$ -subunits from rat atria and the differential regulation of their expression by IGF-I. *J Mol Cell Cardiol* 35:207–215.
- Conti M. 2004. Targeting  $K^+$  channels for cancer therapy. *J Exp Ther Oncol* 4:161–166.
- Dabrosin C. 2003. Increase of free insulin-like growth factor-1 in normal human breast in vivo late in the menstrual cycle. *Breast Cancer Res Treat* 80:193–198.
- Dufourny B, Alblas J, Van Teeffelen HA, Van Schaik FM, Van der Burg B, Steenbergh PH, Sussenbach JS. 1997. Mitogenic signaling of insulin-like growth factor I in MCF-7 human breast cancer cells requires phosphatidylinositol 3-kinase and is independent of mitogen-activated protein kinase. *J Biol Chem* 272:31163–31171.
- Dupont J, Karas M, LeRoith D. 2000. The potentiation of estrogen on insulin-like growth factor I action in MCF-7 human breast cancer cells includes cell cycle components. *J Biol Chem* 275:35893–35901.
- Farias LM, Ocana DB, Diaz L, Larrea F, Avila-Chavez E, Cadena A, Hinojosa LM, Lara G, Villanueva LA, Vargas C, Hernandez-Gallegos E, Camacho-Arroyo I, Duenas-Gonzalez A, Perez-Cardenas E, Pardo LA, Morales A, Taja-Chayeb L, Escamilla J, Sanchez-Pena C, Camacho J. 2004. Ether a go-go potassium channels as human cervical cancer markers. *Cancer Res* 64:6996–7001.
- Fletcher O, Gibson L, Johnson N, Altmann DR, Holly JM, Ashworth A, Peto J, Silva Idos S. 2005. Polymorphisms and circulating levels in the insulin-like growth factor system and risk of breast cancer: A systematic review. *Cancer Epidemiol Biomarkers Prev* 14:2–19.
- Franke TF, Yang SI, Chan TO, Datta K, Kazlauskas A, Morrison DK, Kaplan DR, Tschichnig P. 1995. The protein kinase encoded by the Akt proto-oncogene is a target of the PDGF-activated phosphatidylinositol 3-kinase. *Cell* 81:727–736.
- Gamper N, Fillon S, Huber SM, Feng Y, Kobayashi T, Cohen P, Lang F. 2002. IGF-I up-regulates  $K^+$  channels via PI3-kinase, PDK1 and SGK1. *Pflugers Arch* 43:625–634.
- Gavrilova-Ruch O, Schonherr K, Gessner G, Schonherr R, Klapperstuck T, Wohlrab W, Heinemann SH. 2002. Effects of imipramine on ion channels and proliferation of IGR1 melanoma cells. *J Membr Biol* 188:137–149.
- Gresch O, Engel FB, Nestic D, Tran TT, England HM, Hickman ES, Korner I, Gan L, Chen S, Castro-Obregon S, Hammermann R, Wolf J, Muller-Hartmann H, Nix M, Siebenkotten G, Kraus G, Lun K. 2003. New non-viral method for gene transfer into primary cells. *Methods* 33:151–163.
- Guo W, Kamiya K, Hojo M, Kodama I, Toyama J. 1998. Regulation of  $Kv4.2$  and  $Kv1.4 K^+$  channel expression by myocardial hypertrophic factors in cultured newborn rat ventricular cells. *J Mol Cell Cardiol* 30:1449–1455.
- Guo TB, Lu J, Li T, Xu G, Xu M, Lu L, Dai W. 2005. Insulin-activated,  $K^+$ -channel-sensitive Akt pathway is primary mediator of ML-1 cell proliferation. *Am J Physiol Cell Physiol* 289:257–263.
- Gurney AM, Hunter E. 2005. The use of small interfering RNA to elucidate the activity and function of ion channel genes in an intact tissue. *J Pharmacol Toxicol Methods* 51:253–262.
- Hadsell DL. 2003. The insulin-like growth factor system in normal mammary gland function. *Breast Dis* 17:3–14.
- Hadsell DL, Greenberg NM, Fligger JM, Baumrucker CR, Rosen JM. 1996. Targeted expression of des(1–3) human insulin-like growth factor I in transgenic mice influences mammary gland development and IGF-binding protein expression. *Endocrinology* 137:321–330.
- Hamelers IH, van Schaik RF, Sipkema J, Sussenbach JS, Steenbergh PH. 2002. Insulin-like growth factor I triggers nuclear accumulation of cyclin D1 in MCF-7S breast cancer cells. *J Biol Chem* 277:47645–47652.
- Hankinson SE, Schernhammer ES. 2003. Insulin-like growth factor and breast cancer risk: Evidence from observational studies. *Breast Dis* 17:27–40.
- Hankinson SE, Willett WC, Colditz GA, Hunter DJ, Michaud DS, Deroo B, Rosner B, Speizer FE, Pollak M. 1998. Circulating concentrations of insulin-like growth factor-I and risk of breast cancer. *Lancet* 351:1393–1396.
- Harir N, Pecquet C, Kerenyi M, Sonneck K, Kovacic B, Nyga R, Brevet M, Dhennin I, Gouilleux-Gruart V, Beug H, Valent P, Lassoué K, Moriggi R, Gouilleux F. 2007. Constitutive activation of Stat5 promotes its cytoplasmic localization and association with PI 3-kinase in myeloid leukemias. *Blood* 109:1678–1686.
- Hemmerlein B, Weseloh RM, Mello de Queiroz F, Knotgen H, Sanchez A, Rubio ME, Martin S, Schliephacke T, Jenke M, Radzun HJ, Stuhmer W, Pardo LA. 2006. Overexpression of Eag1 potassium channels in clinical tumours. *Mol Cancer* 5:41–53.
- Ibrahim YH, Yee D. 2004. Insulin-like growth factor-I and cancer risk. *Growth Horm IGF Res* 14:261–269.
- Jackson JG, White MF, Yee D. 1998. Insulin receptor substrate-1 is the predominant signaling molecule activated by insulin-like growth factor-I, insulin, and interleukin-4 in estrogen receptor-positive human breast cancer cells. *J Biol Chem* 273:9994–10003.
- Jones JL, Clemmons DR. 1995. Insulin-like growth factors and their binding proteins: Biological actions. *Endocr Rev* 15:3–34.
- Krosil J, Austin P, Beslu N, Kroon E, Humphries RK, Sauvageau G. 2003. In vitro expansion of hematopoietic stem cells by recombinant TAT-HOXB4 protein. *Nat Med* 9:1428–1432.
- Laban C, Bustin SA, Jenkins PJ. 2003. The GH-IGF-I axis and breast cancer. *Trends Endocrinol Metab* 14:28–34.
- Mello de Queiroz F, Suarez-Kurtz G, Stuhmer W, Pardo LA. 2006. Ether a go-go potassium channel expression in soft tissue sarcoma patients. *Mol Cancer* 5:42–52.
- Meyer R, Schonherr R, Gavrilova-Ruch O, Wohlrab W, Heinemann SH. 1999. Identification of ether a go-go and calcium-activated potassium channels in human melanoma cells. *J Membr Biol* 171:107–115.
- Niemeyer BA, Mery L, Zawar C, Suckow A, Monje F, Pardo LA, Stuhmer W, Flockerzi V, Hoth M. 2001. Ion channels in health and disease. *EMBO Rep* 2:568–573.
- O'Grady SM, Lee SY. 2005. Molecular diversity and function of voltage-gated ( $Kv$ ) potassium channels in epithelial cells. *Int J Biochem Cell Biol* 37:1578–1594.
- Ouadid-Ahidouch H, Le Bourhis X, Roudbaraki M, Toillon RA, Delcourt P, Prevarskaya N. 2001. Changes in the  $K^+$  current-density of MCF-7 cells during progression through the cell cycle: Possible involvement of a h-ether-a-gogo  $K^+$  channel. *Receptors Channels* 7:345–356.

- Ouadid-Ahidouch H, Roudbaraki M, Delcourt P, Ahidouch A, Joury N, Prevarskaya N. 2004. Functional and molecular identification of intermediate-conductance  $\text{Ca}(2+)$ -activated  $\text{K}(+)$  channels in breast cancer cells: Association with cell cycle progression. *Am J Physiol Cell Physiol* 287:125–134.
- Pardo LA, Del Camino D, Sanchez A, Alves F, Bruggemann A, Beckh S, Stuhmer W. 1999. Oncogenic potential of EAG  $\text{K}(+)$  channels. *EMBO J* 18:5540–5547.
- Pardo LA, Contreras-Jurado C, Zientkowska M, Alvares F, Stuhmer W. 2005. Role of voltage-gated potassium channels in cancer. *J Membr Biol* 205:115–124.
- Pollak M. 2000. Insulin-like growth factor physiology and cancer risk. *Eur J Cancer* 36:1224–1228.
- Shen MR, Lin AC, Hsu YM, Chang TJ, Tang MJ, Alper SL, Ellory C, Chou CY. 2004. Insulin-like growth factor I stimulates  $\text{KCl}$  cotransport, which is necessary for invasion and proliferation of cervical cancer and ovarian cancer cells. *J Biol Chem* 279:40017–40025.
- Skolnik EY, Lee CH, Batzer A, Vicentini LM, Zhou M, Daly R, Myers MJ, Jr., Backer JM, Ullrich A, White MF. et al. 1993. The SH2/SH3 domain-containing protein GRB2 interacts with tyrosine-phosphorylated IRS1 and Shc: Implications for insulin control of ras signalling. *EMBO J* 12:1929–1936.
- Surmacz E. 2000. Function of the IGF-I receptor in breast cancer. *J Mammary Gland Biol Neoplasia* 5:95–105.
- Surmacz E, Guvakova MA, Nolan MK, Nicosia RF, Sciacca L. 1998. Type I insulin-like growth factor receptor function in breast cancer. *Breast Cancer Res Treat* 47:255–267.
- Van der Burg B, Rutteman GR, Blankenstein MA, de Laat SW, van Zoelen EJ. 1988. Mitogenic stimulation of human breast cancer cells in a growth factor-defined medium: Synergistic action of insulin and estrogen. *J Cell Physiol* 134:101–108.
- Vocero-Akbani A, Chellaiah MA, Hruska KA, Dowdy SF. 2001. Protein transduction: Delivery of Tat-GTPase fusion proteins into mammalian cells. *Methods Enzymol* 332:36–49.
- Wang Z. 2004. Roles of  $\text{K}^+$  channels in regulating tumour cell proliferation and apoptosis. *Pflugers Arch* 448:274–286.
- Weber C, Mello de Queiroz F, Downie BR, Suckow A, Stuhmer W, Pardo LA. 2006. Silencing the activity and proliferative properties of the human Eagl potassium channel by RNA interference. *J Biol Chem* 281:13030–13037.
- Wei Y, Chen YJ, Li D, Gu R, Wang WH. 2004. Dual effect of insulin-like growth factor on the apical 70-pS  $\text{K}$  channel in the thick ascending limb of rat kidney. *Am J Physiol Cell Physiol* 286:C1258–C1263.
- Wonderlin WF, Strobl JS. 1996. Potassium channels, proliferation and G1 progression. *J Membr Biol* 154:91–107.
- Xu D, Wang L, Dai W, Lu L. 1999. A requirement for  $\text{K}^+$ -channel activity in growth factor-mediated extracellular signal-regulated kinase activation in human myeloblastic leukaemia ML-1 cells. *Blood* 94:139–145.
- Zheng Z, Wang ZM, Delbono O. 2004.  $\text{Ca}^{2+}$ -calmodulin kinase and calcineurin mediate IGF-I-induced skeletal muscle dihydropyridine receptor  $\alpha(1\text{S})$  transcription. *J Membr Biol* 197:101–112.